Optimizing Yb concentration of fiber amplifiers in the presence of transverse modal instabilities and photodarkening

Lægsgaard, Jesper

Published in:
Applied Optics

Link to article, DOI:
10.1364/AO.55.001966

Publication date:
2016

Document Version
Peer reviewed version

Optimizing Yb concentration of fiber amplifiers in the presence of transverse modal instabilities and photodarkening

Jesper Lægsgaard[1]

[1]*DTU Fotonik, Department of Photonics Engineering, Technical University of Denmark, Ørsteds Plads 343, DK-2800 Kongens Lyngby, Denmark*

compiled: June 7, 2016

The Yb concentration of double-clad optical fiber amplifiers is numerically optimized with respect to maximizing the transverse modal instability threshold in the presence of absorption arising from photodarkening. The pump cladding area is scaled with the Yb concentration to approximately maintain the pump absorption in operation. It is found that approximate analytical expressions can predict the optimized concentration levels found in numerical simulations with sufficient accuracy to be useful in fiber design.

OCIS codes: (140.3510) Lasers, Fiber; (140.6810) Lasers, Thermal effects; (060.2320) Fiber optics amplifiers and oscillators; (160.5690) Rare-earth-doped materials.

http://dx.doi.org/10.1364/XX.99.099999

1. Introduction

Transverse modal instabilities (TMI) are currently the main limiting factor for average-power scaling of Yb-doped fiber amplifier systems with large cores [1, 2]. It is by now broadly accepted that thermo-optic nonlinear coupling between the fundamental mode (FM) and first higher-order mode (HOM) of the fiber is the main cause of TMI, and models on various levels of sophistication have been presented [2–7]. An additional issue is the occurence of induced signal absorption, so-called photodarkening (PD), upon prolonged laser operation [8]. Since extra absorption implies an additional heat load, the onset of PD is found to reduce the TMI power threshold [7, 9].

It has been shown by several authors that the TMI induced by the heat load from a given optical gain is reduced by inversion saturation [10, 11]. Therefore, this source of TMI can be diminished by increasing the Yb concentration, N_{Yb}, while maintaining the value of the signal gain. The latter is important because a short amplifier length is often desired to mitigate nonlinear effects, such as self-phase modulation or Raman scattering. On the other hand, PD effects approximately increase with N_{Yb}^2 [7, 12], so N_{Yb} may be expected to have an optimum value with respect to maximization of the TMI threshold.

The purpose of this work is to numerically study the optimization of Yb doping concentrations in a double-clad step-index fiber amplifier. Analytical expressions for the optimal concentration are derived from simplified assumptions and compared to results of the numerical simulations. The expressions are found to give useful predictions for optimal N_{Yb} values when taking the variation of TMI threshold with N_{Yb} into account.

The paper is organized as follows: In section 2, the numerical model for calculating the TMI threshold is laid out, and an approximate analytical estimation of the optimal Yb concentration is derived. In section 3, numerical results are presented for optimal Yb concentrations, and the corresponding threshold powers, and comparison is made to the analytical estimate. Section 4 summarizes the conclusions.

2. Formal theory

The simplified model of TMI proposed in refs. [11, 13] is adopted, in an undepleted-pump approximation, for the numerical simulations. The power evolution in the fundamental and higher or-

der modes, $P_1(z)$, $P_2(z)$, is in this model given by

$$\frac{dP_1}{dz} = \Gamma_1(z)P_1(z) \quad (1)$$

$$\frac{dP_2}{dz} = \left[\Gamma_2(z) + \chi_2(z,\Omega)P_1(z)\right] P_2(z,\Omega) \quad (2)$$

$$\Gamma_i(z) = 2\pi \int_0^{r_d} dr R_i^2(r) \left[\frac{g_0(z)}{1+\frac{I_s(r,z)}{I_{sat}(z)}} - \gamma_{PD}(r,z) \right] \quad (3)$$

$$g_0(z) = N_{Yb} \frac{I_p(z)(\sigma_{ap}\sigma_{es} - \sigma_{as}\sigma_{ep}) - P_\tau \sigma_{as}}{I_p(z)(\sigma_{ap}+\sigma_{ep}) + P_\tau} \quad (4)$$

$$I_{sat}(z) = \frac{\omega_s}{\omega_p} \frac{I_p(z)(\sigma_{ap}+\sigma_{ep}) + P_\tau}{\sigma_{as}+\sigma_{es}} \quad (5)$$

$$I_s(r,z) = P_1(z)R_1^2(r);\ P_\tau = \frac{\hbar\omega_p}{\tau};\ I_p(z) = \frac{P_p(z)}{A_p} \quad (6)$$

Here σ_{as}, σ_{ap}, σ_{es}, σ_{ep} are absorption and emission cross sections for signal and pump respectively, ω_p, ω_s are the pump and signal frequencies respectively, τ the Yb upper-state lifetime, and Ω the frequency detuning between the signals in the fundamental and higher-order mode, typically in the kHz range. The doping radius of the core is denoted r_d, and a uniform Yb-distribution inside this radius is assumed. In the present work, the core radius is taken to be equal to r_d, but this is not a necessary requirement. A_p is the area of the pump core, or inner cladding. The radial guided-mode profiles R_i are normalized so that

$$2\pi \int_0^\infty dr R_i^2(r) = 1. \quad (7)$$

Assuming backward pumping, the pump power $P_p(z)$ obeys the evolution equation

$$\frac{dP_p}{dz} = \frac{2\pi N_{Yb}}{A_p} \int_0^{r_d} dr \left[\sigma_{ap} - n_2(r,z)(\sigma_{ap}+\sigma_{ep})\right] \quad (8)$$

with $n_2(r,z)$ given by

$$n_2(r,z) = \frac{g_0(z)}{N_{Yb}(\sigma_{as}+\sigma_{es})\left(1+\frac{I_s(r,z)}{I_{sat}(z)}\right)} + \frac{\sigma_{as}}{\sigma_{as}+\sigma_{es}} \quad (9)$$

In writing Eq. (1) it has been assumed that $P_2 << P_1$ holds everywhere, so that the depletion of P_1 by the coupling term in Eq. (2) can be neglected. By the same assumption, the signal intensity I_s is calculated from P_1 only.

The absorption from photodarkening (PD) is described by γ_{PD}, whose asymptotic value in long-term use of the amplifier at a specific inversion level is assumed to be

$$\gamma_{PD}(r,z) = \alpha_{PD} N_{Yb}^2 n_2(r,z) \quad (10)$$

While this model is in reasonable, though not perfect, accord with various published data, the magnitude of reported PD effects vary widely across the literature. For this reason, α_{PD} will in this work be taken as a variable parameter, whose order of magnitude will be discussed in section 3.

The crucial nonlinear coupling parameter $\chi_2(z,\Omega)$ is given by

$$\chi_2(z,\Omega) = 2\pi \frac{\eta\omega_p}{c\kappa n_0} \int_0^\infty dr R_1(r)R_2(r) \int_0^{r_d} dr' q(z,r') \mathrm{Im}\left[g_1(r,r',\Omega)\right] R_1(r')R_2(r') \quad (11)$$

$$q(z,r') = \frac{g_0(z)\left(\frac{\omega_p}{\omega_s}-1\right)}{\left(1+\frac{I_s(r',z)}{I_{sat}(z)}\right)^2} + \gamma_{PD}(r,z) \quad (12)$$

where $g_1(r,r',\Omega)$ is the m=1 component of the Greens function that solves the steady-periodic heat transfer problem at the frequency Ω, as given in [3].

The above equations are solved numerically to estimate the TMI threshold in a given amplifier layout. The threshold is determined by requiring that the total HOM power, integrated over the Ω range where χ_2 is appreciable, is below 10 per cent of the FM power when seeding the HOM with quantum noise (one photon per frequency bin). The threshold power is only weakly dependent on the exact choice of this criterion. As discussed in other works, the threshold is reduced if the HOM is seeded by amplitude noise [6], but this is of little consequence for the N_{Yb} optimization which is the central purpose of this paper.

To obtain an analytical estimate for the optimal N_{Yb}, the following approximations are made: i) The transverse variation of the guided mode profile is neglected, so the signal intensity becomes $I_s(r,z)=I_s(z)=\frac{P_1 O_1}{A_d}$, where O_1 is the overlap integral of the FM with the doped area A_d. ii) $P_\tau \approx 0$ is used to simplify Eqs. (4), writing $g_0 \approx N_{Yb}(\sigma_{ap}\sigma_{es}-\sigma_{as}\sigma_{ep})/(\sigma_{ap}+\sigma_{ep})$. iii) The saturated gain, $g_s = g_0/(1+P_1/P_{sat})$ is approximated to be constant along the amplifier, with $P_{sat}=\frac{I_{sat}A_d}{O_1}$.

Under these assumptions, one finds for n_2 and the total gain for the HOM going through the amplifier,

G_2:

$$n_2 = \frac{g_s + N_{Yb}\sigma_{as}}{N_{Yb}(\sigma_{as}+\sigma_{es})} \tag{13}$$

$$G_2(\Omega) = g_s O_2 L + \tilde{\chi}_2(\Omega)\Bigg\{ \frac{\left(\frac{\omega_p}{\omega_s}-1\right) g_0}{\left(1+\frac{P_1}{P_{sat}}\right)^2} + \alpha_{PD} N_{Yb}^2 n_2 \Bigg\} \int_0^L dz P_1(z) =$$

$$g_s O_2 L + \tilde{\chi}_2(\Omega)\Bigg\{ \left(\frac{\omega_p}{\omega_s}-1\right)\frac{g_s^2}{g_0} + \frac{\alpha_{PD} N_{Yb} g_s}{(\sigma_{as}+\sigma_{es})}\left(1+\frac{N_{Yb}\sigma_{as}}{g_s}\right)\Bigg\}\frac{\Delta P_1}{g_s O_1} \tag{14}$$

$$\tilde{\chi}_2(\Omega) = 2\pi\frac{\eta\omega_p}{c\kappa n_0}\int_0^\infty dr R_1(r)R_2(r) \int_0^{r_d} dr' \mathrm{Im}\left[g_1(r,r',\Omega)\right] R_1(r')R_2(r') \tag{15}$$

where O_2 is the HOM overlap with the doped area and L is the amplifier length. ΔP_1 is the difference between output and input signal power, and it was utilized in evaluating the z-integral that the constant FM signal gain is given by $g_s O_1$. The direct contribution of PD loss to the gain has been omitted, as it is expected to be neglibible compared to the change it induces in the TMI gain.

Since the magnitude of the signal gain is not known *a priori*, a final approximation is made: iv) $g_s O_1 = \alpha_p$, where α_p is the pump absorption in operation. Using Eq. (13), this assumption yields

$$\alpha_p = N_{Yb}\left(\sigma_{ap} - n_2(\sigma_{ap}+\sigma_{ep})\right)\frac{A_d}{A_p} = N_{Yb}\left(\sigma_{ap} - \frac{\frac{\alpha_p}{O_1}+N_{Yb}\sigma_{as}}{N_{Yb}(\sigma_{as}+\sigma_{es})}(\sigma_{ap}+\sigma_{ep})\right)\frac{A_d}{A_p}$$

$$\Downarrow$$

$$\frac{A_d}{A_p} = \frac{\alpha_p(\sigma_{as}+\sigma_{es})}{N_{Yb}(\sigma_{es}\sigma_{ap}-\sigma_{as}\sigma_{ep}) - \frac{\alpha_p}{O_1}(\sigma_{ap}+\sigma_{ep})} \tag{16}$$

In the present work α_p and N_{Yb} will be taken as input parameters, using Eq. (16) to determine the radius of the pump cladding. It is important to note that α_p is *not* the small-signal pump absorption, but a design target for the pump absorption in operation. Clearly, the assumption of a certain pump absorption, and in particular a certain signal gain, cannot be true over a wide range of pump powers. For a backward-pumped amplifier, iv) corresponds to photon number conservation if spontaneous emission is negligible, and the unabsorbed pump power is equal to the signal seed power. While the former condition is consistent with ii), the latter will only be exactly fulfilled at a single value of the pump power. Ultimately, the chosen value of α_p should therefore be regarded as expressing a certain scaling relation between N_{Yb} and A_d/A_p, as given by Eq. (16). However, such a scaling is central to the whole idea of optimizing the TMI threshold by reducing the amplifier inversion level. Therefore, in all the numerical investigations presented here, it is understood that A_p is scaled with N_{Yb} according to Eq. (16). Comparison to the numerical calculations will be the ultimate test of the approximate equations derived below.

Inserting assumptions ii), iv) into Eq. (14), one obtains

$$G_2(\Omega) = \tilde{\chi}_2(\Omega)\Bigg\{ \left(\frac{\omega_p}{\omega_s}-1\right)\frac{\alpha_p^2(\sigma_{ap}+\sigma_{ep})}{O_1^2 N_{Yb}(\sigma_{ap}\sigma_{es}-\sigma_{as}\sigma_{ep})} + \frac{\alpha_{PD}N_{Yb}\alpha_p}{O_1(\sigma_{as}+\sigma_{es})}\left(1+\frac{O_1 N_{Yb}\sigma_{as}}{\alpha_p}\right)\Bigg\}\frac{\Delta P_1}{\alpha_p} + \alpha_p\frac{O_2}{O_1}L \tag{17}$$

Equating the N_{Yb}-derivative of Eq. (17) to zero, treating α_p as a constant, leads to the condition

$$\frac{\alpha_p\left(\frac{\omega_p}{\omega_s}-1\right)(\sigma_{ap}+\sigma_{ep})}{(\sigma_{ap}\sigma_{es}-\sigma_{as}\sigma_{ep})O_1^2} = \frac{\alpha_{PD}N_{Yb}^2}{(\sigma_{as}+\sigma_{es})O_1}\left(1+\frac{2\sigma_{as}O_1}{\alpha_p}N_{Yb}\right) \tag{18}$$

This third-order equation is readily solved for N_{Yb}. If $\frac{2\sigma_{as}O_1}{\alpha_p}N_{Yb} << 1$ one has the explicit expression

$$N_{Yb} = \sqrt{\frac{\alpha_p\left(\frac{\omega_p}{\omega_s}-1\right)(\sigma_{ap}+\sigma_{ep})(\sigma_{as}+\sigma_{es})}{\alpha_{PD}(\sigma_{ap}\sigma_{es}-\sigma_{as}\sigma_{ep})O_1}} \tag{19}$$

This approximation is, however, not always accurate, as will be shown in section 3.

3. Numerical results and discussion

In the simulations, an amplifier having L=1 m, a core radius of 20 μm, α_p=10 dB/m, pump wavelength of 976 nm, signal wavelength λ_s=1030 nm, a V-parameter of 4, and input signal power of either 10 or 40 W is used as a reference system. Variations in either α_p, signal wavelength or α_{PD} around their reference values are considered, in order to determine the optimal Yb concentration, N_{opt}, and test the accuracy of Eqs. (18), (19).

The choice of a range for α_{PD} merits some discussion. A parametrization corresponding to $\alpha_{PD} \approx$

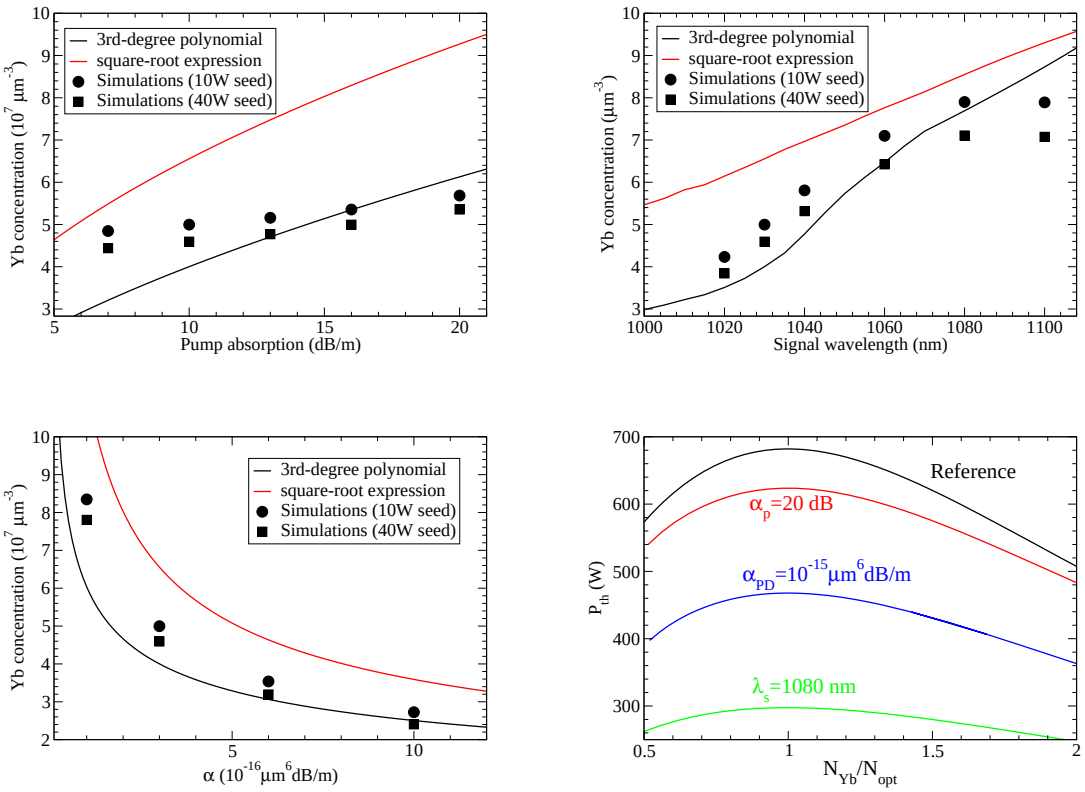

Fig. 1. Optimal N_{Yb}-values as function of α_p (top left), signal wavelength λ_s (top right), and α_{PD} (bottom left). The variation of the TMI threshold P_{th} with deviation from the optimal Yb concentration N_{opt} is illustrated in the bottom right panel for four specific cases.

$2 \cdot 10^{-15} \mu$m^{6}dB/m was recently proposed[7], based on earlier experimental work [12, 14]. On the other hand, Mattsson reported PD loss measurements suggesting an $\alpha_{PD} < 10^{-16} \mu$m^{6}dB/m for a uniform core doping [15]. Other authors have published PD loss measurements in between these extremes [16, 17]. For the calculations in the present work an α_{PD} range of $10^{-15} - 10^{-16} \mu$m^{6}dB/m is therefore considered.

In figure 1, the results of Eqs. (18), (19) are compared to optimal Yb concentrations derived from the numerical simulations, when varying individual parameters as discussed above. Clearly, Eq. (18) is only accurate to typically within 10-30%, with some deviations exceeding 50 %. However, as illustrated by the final plot of selected TMI thresholds versus the deviation of N_{Yb} from its optimum value N_{opt}, these inaccuracies are of minor consequence for the resulting threshold. For instance, a 30% deviation from the optimum N_{Yb} typically leads to a $\sim$5% deviation in TMI threshold. It may also be noted that the dependence of N_{opt} on the seed power, which does not enter into Eqs. (18), (19), is relatively small. Thus, the calculations confirm that the proposed equations are useful for estimating optimal Yb concentrations.

In figure 2, the threshold powers obtained at the optimal values of N_{Yb} are shown for the various cases. It is important to stress that all thresholds plotted are for the optimal value of N_{Yb} as shown in Fig. 1, and with the pump cladding area A_p scaled according to Eq. (16). Therefore the figures cannot be interpreted as showing the effect of varying only a single parameter, such as the signal wavelength. Clearly, a variation of α_p, *i.e.* the relation between N_{Yb} and pump cladding area, has relatively small influence on both the optimal N_{Yb} value, and the resulting threshold. On the other hand, there is a considerable variation with λ_s, with a value around the pump absorption maximum at 1030 nm or even lower being optimal. In addition, as expected, minimization of α_{PD} is crucial for improving the TMI threshold. Also shown in Fig. 2 is a scatter plot displaying all calculated threshold

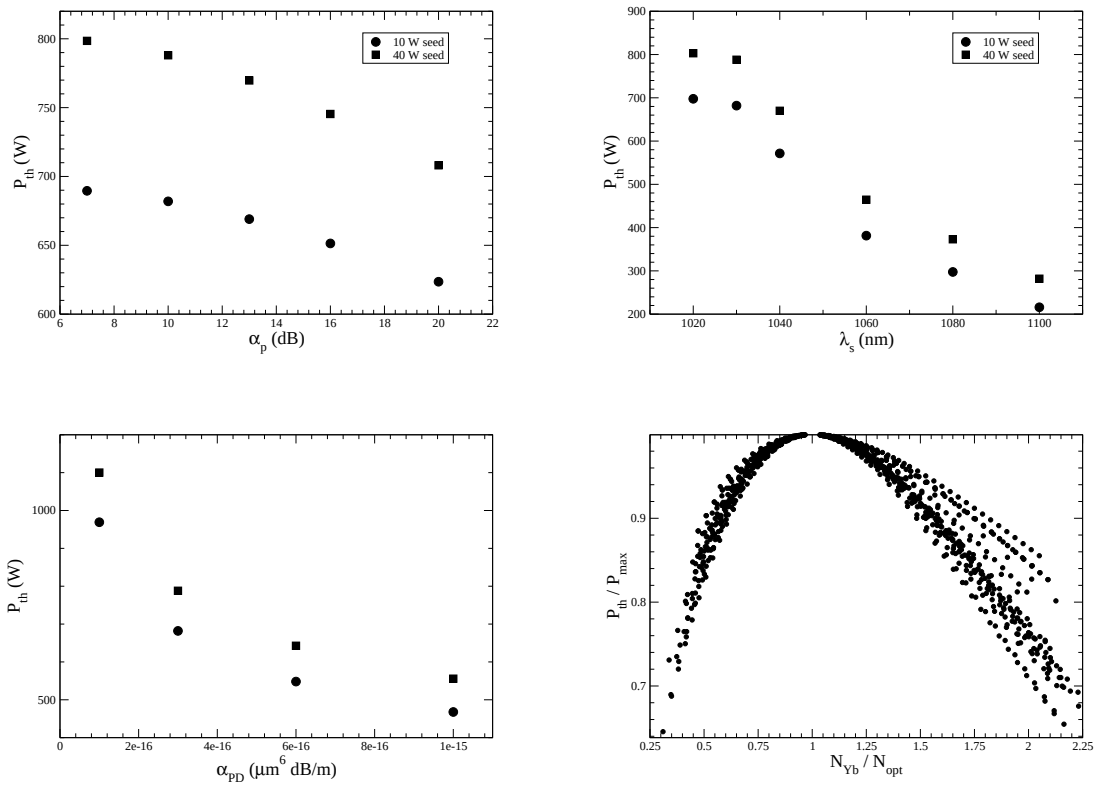

Fig. 2. Threshold power as function of α_p (top left), signal wavelength λ_s (top right), and α_{PD} (bottom left). A scatter plot of threshold power relative to its maximum as a function of N_{Yb} relative to its optimum is shown in the bottom right panel.

powers, each normalized to the threshold power at the optimal value of N_{Yb}, N_{opt}, as a function of N_{Yb}/N_{opt}. The plot shows that a factor-of-two deviation from the optimal value of N_{Yb} will imply a reduction of the threshold power to 70-90% of its maximal value. The sensitivity is found to increase with decreasing α_p, α_{PD} and λ_s, *i.e.* fibers with a high optimized threshold power will also be the most sensitive to variations in N_{Yb}.

It is clear from the simulation results that the material parameter α_{PD} is critical for the calculation. A simple method for estimating this parameter is to compare the TMI threshold of a fresh fiber with that of one in which PD is fully developed under the desired operating conditions. α_{PD} can then be extracted by numerical modelling. An analytical estimate may also be obtained in the spirit of the above derivations. Assuming that the TMI threshold corresponds to a certain level of nonlinear gain, Eq. (14) yields

$$\left(\frac{\omega_p}{\omega_s}-1\right)\frac{g_1}{g_0 O_1^2}\Delta P_{11} = \left(\frac{\omega_p}{\omega_s}-1\right)\left(\frac{g_2}{g_0 O_1^2} + \frac{\alpha_{PD} N_{Yb}}{(\sigma_{as}+\sigma_{es})O_1}\left(1+\frac{N_{Yb}\sigma_{as}O_1}{g_2}\right)\right)\Delta P_{12} \qquad (20)$$

omitting the linear gain term for simplicity. Here g_1, g_2 are the average signal gains (recall that FM signal gain is $g_s O_1$) before and after PD saturation (which in this experiment may be determined from the signal input and output levels), and ΔP_{11}, ΔP_{12} are the ΔP_1 levels before and after PD. Eq. (20) can be rearranged to yield

$$\alpha_{PD} = \frac{\left(\frac{\omega_p}{\omega_s}-1\right)(\sigma_{ap}+\sigma_{ep})(\sigma_{as}+\sigma_{es})}{O_1 N_{Yb}^2(\sigma_{ap}\sigma_{es}-\sigma_{as}\sigma_{ep})(1+\frac{N_{Yb}\sigma_{as}O_1}{g_2})} \times \frac{g_1\Delta P_{11} - g_2\Delta P_{12}}{\Delta P_{12}} \qquad (21)$$

Fig. 3 shows values of α_{PD} calculated from results of numerical simulations using Eq. (21) rel-

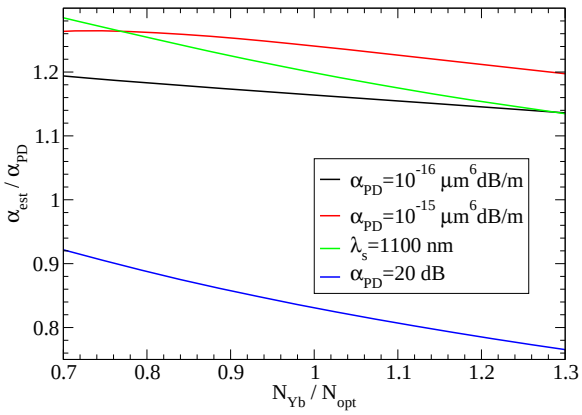

Fig. 3. Estimated α_{PD}-values relative to actual α_{PD} as a function of N_{Yb} relative to optimum N_{Yb}=N_{opt} for four different cases. α_{est} is calculated from Eq. (21) based on output from the numerical simulations.

ative to the actual α_{PD}-value used in the simulations. In all calculations, PD saturation was found to reduce the threshold power to 70-80% of the value in a fresh fiber. The deviation between the simplified formula and the numerical results is on the level of 10-30%. Thus Eq. (21) is useful for a rough estimate, but a detailed simulation is needed for an accurate determination of α_{PD}.

4. conclusion

In conclusion, numerical estimates for the optimal Yb concentration with respect to TMI mitigation in the presence of photodarkening have been presented as a function of PD magnitude, signal wavelength and pump absorption. Simplified equations for predicting optimal Yb concentrations and photodarkening strength have been derived and shown to agree with numerical simulations within $\sim 50\%$. The main assumptions behind the calculations are the dependence of photodarkening strength on Yb concentration and inversion level, Eq. (10), and the validity of the simplified theoretical model. It is also important to note that the simulations were done for a step-index amplifier with a V-parameter of 4, meaning that the LP_{11} mode is reasonably well confined, and not overly sensitive to thermal perturbations. If one consideres fibers which are closer to the single-mode regime, thermally induced changes in the mode profiles [18] could lead to a considerable variation with propagation distance of the overlap integrals determining the thermo-optic nonlinear coupling. In such a case, one may need to consider a more comprehensive numerical and analytical model.

References

[1] T. Eidam, C. Wirth, C. Jauregui, F. Stutzki, F. Jansen, H.-J. Otto, O. Schmidt, T. Schreiber, J. Limpert, and A. Tünnermann, "Experimental observations of the threshold-like onset of mode instabilities in high power fiber amplifiers," Opt. Express **19**, 13218–13224 (2011).

[2] A. V. Smith and J. J. Smith, "Mode instability in high power fiber amplifiers," Opt. Express **19**, 10180–10192 (2011).

[3] K. R. Hansen, T. T. Alkeskjold, J. Broeng, and J. Lægsgaard, "Thermally induced mode coupling in rare-earth doped fiber amplifiers," Opt. Lett. **37**, 2382–2384 (2012).

[4] B. G. Ward, "Modeling of transient modal instability in fiber amplifiers," Opt. Express **21**, 12053–12067 (2013).

[5] L. Dong, "Stimulated thermal rayleigh scattering in optical fibers," Opt. Express **21**, 2642–2656 (2013).

[6] K. R. Hansen, T. T. Alkeskjold, J. Broeng, and J. Lægsgaard, "Theoretical analysis of mode instability in high-power fiber amplifiers," Opt. Express **21**, 1944–1971 (2013).

[7] C. Jauregui, H.-J. Otto, F. Stutzki, J. Limpert, and A. Tünnermann, "Simplified modelling the mode instability threshold of high power fiber amplifiers in the presence of photodarkening," Opt. Express **23**, 20203–20218 (2015).

[8] J. J. Koponen, M. J. Söderlund, H. J. Hoffman, and S. K. T. Tammela, "Measuring photodarkening from single-mode ytterbium doped silica fibers," Opt. Express **14**, 11539–11544 (2006).

[9] M. M. Johansen, M. Laurila, M. D. Maack, D. Noordegraaf, C. Jakobsen, T. T. Alkeskjold, and J. Lægsgaard, "Frequency resolved transverse mode instability in rod fiber amplifiers," Opt. Express **21**, 21847–21856 (2013).

[10] A. V. Smith and J. J. Smith, "Increasing mode instability thresholds of fiber amplifiers by gain saturation," Opt. Express **21**, 15168–15182 (2013).

[11] K. R. Hansen and J. Lægsgaard, "Impact of gain saturation on the mode instability threshold in high-power fiber amplifiers," Opt. Express **22**, 11267–11278 (2014).

[12] S. Taccheo, H. Gebavi, A. Monteville, O. L. Goffic, D. Landais, D. Mechin, D. Tregoat, B. Cadier, T. Robin, D. Milanese, and T. Durrant, "Concentration dependence and self-similarity of photodarkening losses induced in yb-doped fibers by comparable excitation," Opt. Express **19**, 19340–19345 (2011).

[13] R. Tao, P. Ma, X. Wang, P. Zhou, and Z. Liu, "Study of Wavelength Dependence of Mode Insta-

bility Based on a Semi-Analytical Model," IEEE Journal of quantum electronics **51**, 1–6 (2015).

[14] H. Gebavi, S. Taccheo, L. Lablonde, B. Cadier, T. Robin, D. Méchin, and D. Tregoat, "Mitigation of photodarkening phenomenon in fiber lasers by 633 nm light exposure," Opt. Lett. **38**, 196–198 (2013).

[15] K. E. Mattsson, "Photo darkening of rare earth doped silica," Opt. Express **19**, 19797–19812 (2011).

[16] S. Jetschke, S. Unger, U. Röpke, and J. Kirchhof, "Photodarkening in yb doped fibers: experimental evidence of equilibrium states depending on the pump power," Opt. Express **15**, 14838–14843 (2007).

[17] S. Jetschke, S. Unger, A. Schwuchow, M. Leich, and J. Kirchhof, "Efficient yb laser fibers with low photodarkening by optimization of the core composition," Opt. Express **16**, 15540–15545 (2008).

[18] F. Jansen, F. Stutzki, H.-J. Otto, T. Eidam, A. Liem, C. Jauregui, J. Limpert, and A. Tuennermann, "Thermally induced waveguide changes in active fibers," Opt. Express **20**, 3997–4008 (2012).